

Consideration about vertical laplacian operator being discretized using VFE

Jozef Vivoda

June 6, 2014

1 Formulation

This short note is analysis of properties of vertical linear laplacian operator discretized with finite element method.

The eigenvalues of discrete laplacian must be real and negative in order to ensure the stable time stepping with Crank-Nicholson scheme (centered implicit scheme).

2 Laplacian in mass based coordinate system

Linear vertical laplacian operator in mass coordinate $\pi = A(\eta) + B(\eta)\pi_s$ is

$$form1 : \mathbf{L}^* X = \frac{\pi^*}{m^*} \frac{\partial}{\partial \eta} \left(\frac{\pi^*}{m^*} \frac{\partial}{\partial \eta} + 1 \right) \hat{q} \quad (1)$$

resp.

$$form2 : \mathbf{L}^* X = \frac{1}{m^*} \frac{\partial}{\partial \eta} \left(\frac{\pi^{*2}}{m^*} \right) \frac{\partial \hat{q}}{\partial \eta} + \left(\frac{\pi^*}{m^*} \right)^2 \frac{\partial^2 \hat{q}}{\partial \eta^2} \quad (2)$$

with $m^* = \frac{\partial \pi^*}{\partial \eta}$ and $\hat{q} = \log \frac{p}{\pi}$.

3 Finite element method

We discretized derivative, second derivative and integral operator. We use notation $g(f(\eta))$ for general representation of these operators. We discretize the differential form

$$g(f(\eta)) = d(\eta) \quad (3)$$

We expand $f(\eta) = \sum_{i=1}^L \hat{f}_i B_i(\eta)$ and $d(\eta) = \sum_{i=1}^L \hat{d}_i D_i(\eta)$. Having $f(\eta)$ sampled on L model levels, we can transform it from physical to VFE space as $f(\eta_k) = \sum_{i=1}^L \hat{f}_i B_i(\eta_k)$. The same holds for $d(\eta)$.

We use two independent set of spline basis functions B and D . When we substitute these expansions into differential form we obtain

$$\sum_{i=1}^L \hat{\mathbf{f}}_i \mathbf{g}(\mathbf{B}_i(\eta)) = \sum_{i=1}^L \hat{\mathbf{d}}_i \mathbf{D}_i(\eta). \quad (4)$$

Weak form of differential form is obtained with arbitrary set of L weighting functions w

$$\sum_{i=0}^{L+1} \left[\int_0^1 \mathbf{g}(\mathbf{B}_i(\eta)) \mathbf{w}_j(\eta) d\eta \right] \hat{f}_i = \sum_{i=0}^{L+1} \left[\int_0^1 \mathbf{D}_i(\eta) \mathbf{w}_j(\eta) d\eta \right] \hat{d}_i \quad j = 1, \dots, L. \quad (5)$$

Spline basis functions B , D and w are independent. When we put $B = D = w$ then the method leads to Galerkin method. We investigate Galerkin method in following sections.

4 Finite element discretisation with B-splines and regular vertical σ levels

The sigma coordinate is limit case of η coordinate when $A(\eta) = 0$ and $\sigma = \frac{\pi}{\pi_s}$.

The laplacian operator in σ coordinate is

$$form1: \quad \mathbf{L}^* X = \sigma \frac{\partial}{\partial \sigma} \left(\sigma \frac{\partial}{\partial \sigma} + 1 \right) \hat{q} \quad (6)$$

resp.

$$form2: \quad \mathbf{L}^* X = \sigma \left(2 \frac{\partial}{\partial \sigma} + \sigma \frac{\partial^2}{\partial \sigma^2} \right) \hat{q}. \quad (7)$$

Vertical domain is sampled with L regular layers. The interfaces between layers are half levels with $\sigma_l = \frac{l}{L}, l \in (0, \dots, L)$. Full levels are in the middle of layers with $\sigma_l = \frac{\sigma_l + \sigma_{l-1}}{2}, l \in (1, \dots, L)$.

The eigenvalues of FE discretized laplacian operator are analyzed with respect to chosen boundary conditions (BCs). The BCs are incorporated into basis functions by controlling the multiplicity of boundary knot sequence.

The general spline basis of order C is defined using internal knots sequence $t_i = \sigma_{i+\frac{C}{2}}, i \in 1, \dots, L - C$. The knots sequence is further completed by boundary knots with multiplicity C at model top and model surface. When we require

boundary condition $B_i = 0, i \in (0, \dots, L)$ at some boundary we simply decrease the multiplicity of knot by 1 at that boundary and move that knot into internal domain. When we require boundary condition $(\frac{\partial B}{\partial \sigma})_i = 0, i \in (0, \dots, L)$ at some boundary we decrease the multiplicity of knot by 2 at that boundary and move those 2 knots into internal domain.

We define following 5 sets of basis functions

- noBCs general spline basis with multiplicity of knots at boundaries C . The knot sequence of cubic spline basis ($C = 4$) and regular 5 levels is $t = (0, 0, 0, 0, \frac{1}{2}, 1, 1, 1, 1)$. The basis is plotted at Figure 1 (a).
- TBC0 spline basis with $B_i(\sigma = 0) = 0, i \in (0, \dots, L)$. Multiplicity of top knot is $C - 1$. The knot sequence of cubic spline basis ($C = 4$) and regular 5 levels is $t = (0, 0, 0, \frac{3}{10}, \frac{1}{2}, 1, 1, 1, 1)$. The basis is plotted at Figure 1 (b).
- BBC0 spline basis with $B_i(\sigma = 1) = 0, i \in (0, \dots, L)$. Multiplicity of surface knot is $C - 1$. The knot sequence of cubic spline basis ($C = 4$) and regular 5 levels is $t = (0, 0, 0, 0, \frac{1}{2}, \frac{7}{10}, 1, 1, 1)$. The basis is plotted at Figure 1 (c).
- TBCD0 spline basis with $(\frac{\partial B}{\partial \sigma})_i(\sigma = 0) = 0, i \in (0, \dots, L)$. Multiplicity of top knot is $C - 2$. The knot sequence of cubic spline basis ($C = 4$) and regular 5 levels is $t = (0, 0, \frac{1}{10}, \frac{3}{10}, \frac{1}{2}, 1, 1, 1, 1)$. The basis is plotted at Figure 1 (d).
- BBCD0 spline basis with $(\frac{\partial B}{\partial \sigma})_i(\sigma = 1) = 0, i \in (0, \dots, L)$. Multiplicity of surface knot is $C - 2$. The knot sequence of cubic spline basis ($C = 4$) and regular 5 levels is $t = (0, 0, 0, 0, \frac{1}{2}, \frac{7}{10}, \frac{9}{10}, 1, 1)$. The basis is plotted at Figure 1 (e).

The respective eigenvalues of VFE discretized laplacian equivalent of form1 [6] resp. form2 [7] are plotted in complex plane on Figure 2. We see that only form2 with BBC $B_i(\sigma = 1) = 0, i \in (0, \dots, L)$ and $(\frac{\partial B}{\partial \sigma})_i(\sigma = 1) = 0, i \in (0, \dots, L)$ leads to real and negative eigenvalues.

We conclude that due to stability requirements we have to use in FE discretized vertical laplacian operator boundary condition $B(\sigma = 1) = 0$ or $\frac{\partial B}{\partial \sigma}(\sigma = 1) = 0$.

Further we will investigate discretisation of form2 only with proper BBC.

5 Finite element discretisation with B-splines. Position of knots and regularity of σ levels.

In previous section we assumed definition of knots derived from full levels values of σ . Now we define knot sequence differently as $t_i = \sin(\frac{\pi i}{2L}), i = 1 + \frac{C}{2}, L - \frac{C}{2} + 1$. Corresponding basis functions and eigenvalues of laplacian operator for 5 levels are on Figure 3. The eigenvalues are complex.

We assume that knot sequence must be chosen consistent with full level values of σ in order to ensure laplacian eigenvalues to be real and negative.

Further we investigate non-regular level distribution $\sigma_{\tilde{l}} = \left(\frac{\tilde{l}}{L}\right)^{0.1}$, $\tilde{l} \in (0, \dots, L)$. Full levels are still averages of half levels. The internal knots are consistent with definition of full levels $t_i = \sigma_{i+\frac{C}{2}}$, $i \in 1, \dots, L - C + 1$. Multiplicity of knot at model bottom is $C - 1$ for proper BBC treatment. Distribution of levels is very sparse at model top and extremely dense near model surface. Corresponding basis functions and eigenvalues of laplacian operator for 5 levels are on Figure 4. We see that the laplacian eigenvalues are real and negative even for this highly non-regular distribution of vertical levels.

We investigate another non-regular definition $\sigma_{\tilde{l}} = \left(\frac{\tilde{l}}{L}\right)^3$, $\tilde{l} \in (0, \dots, L)$. The levels close to model top are much denser than those close to model surface. Corresponding basis functions and eigenvalues of laplacian operator for 5 levels are on Figure 5. We see that the laplacian eigenvalues are complex.

We conclude that the levels must be regular resp. denser towards the bottom half of model domain. However, we did not find any explicit relationship between the half/full levels distribution and eigenvalues of FE discretized laplacian operator. This issue remains opened.

6 Basis and weighting functions

Here we will relax Galerking method and we will assume that basis functions B , D and w are different. We will investigate how setting zero BBC in each of them influences laplacian eigenvalues.

All tests in this section used regular σ levels distribution. Only one of spline basis was defined with investigated BBC. The eigenvalues for 5 levels are plotted on Figure 6. The real and negative eigenvalues are obtained only, when zero BBC is introduced to basis functions B . These are basis functions of input function. This means that theoretically linear laplacian shall be applied on quantity which holds this condition.

There is first and second derivative operator in laplacian. We will now apply zero BBC at input spline basis B independently on each. Results are shown on Figure 7. We see that crucial condition seems to be the the BBC for first derivative operator in laplacian term.

7 Analysis of eigenvalues of VFE laplacian in η coordinate

We start with the continuous definition of implicit vertical coordinate η

$$\pi(\eta) = \tilde{A}(\eta)\pi_{ref} + B(\eta)\pi_s. \quad (8)$$

We introduced $\tilde{A}(\eta) = \frac{A(\eta)}{\pi_{ref}}$ with π_{ref} being auxiliary constant. Usually we set $\pi_{ref} = 101325Pa$. Our coordinate is implicit, but for the purpose of finite element method must be explicitly defined. We adopt following definition

$$\eta = \tilde{A}(\eta) + B(\eta). \quad (9)$$

It ensures that η converges towards σ in the sense that when $\pi_{ref} = \pi_s$ then $\frac{\partial\pi(\eta)}{\partial\eta} = \pi_s$ as in the case of σ . Therefore η can be seen as a departure from σ coordinate due to difference between π_{ref} and π_s .

We have to realize the limitation of η . The vertical derivative of π must hold $\frac{\partial\pi}{\partial\eta} > 0$ for any values of π_s with fixed π_{ref} . Physical it means that mass must be decreasing with height.

We define \tilde{A} and B (proposal of Jan Masek) in the following way

$$\tau = (3 - 2\eta)\eta^2 \quad (10)$$

$$B = \eta\tau \quad (11)$$

$$\tilde{A} = \eta(1 - \tau). \quad (12)$$

We can easily check that this choice holds [9]. The functions are plotted on Figure 8.

This definition satisfies $\frac{\partial\pi}{\partial\eta} > 0$ for all surface pressures $\pi_s > 41281Pa$. This limiting value of surface pressure is further denoted as π_{min} . Taking into account that the surface pressure at Mount Everest as approx. $30000Pa$, we can not use this definition for high resolution global model. However, it is sufficiently representative for the purpose of this analysis.

The minimum surface pressure π_{min} that satisfy condition $\frac{\partial\pi}{\partial\eta} > 0$ is the solution of $\frac{\partial^2\pi}{\partial\eta^2} = 0$ on interval $0 \leq \eta \leq 1$.

The discrete values of η are defined at half levels in the same manner as σ in sections above

$$\eta_i = \left(\frac{i}{L}\right)^\gamma, i = (0, \dots, L). \quad (13)$$

We consider the case $\gamma = 0.3$. This means that the model levels are non-regular with increasing density towards surface. We present result for 15 level sampling in this section (we found empirically that analysis with 5 levels is not sufficient).

Cubic spline basis with $B_{surf} = 0$ in the both derivative operators was used. This ensures the correct eigenvalues of laplacian in the case that $\eta \rightarrow \sigma$ (see above sections).

We have computed the eigenvalues of FE discretized operator for $\pi_{min} < \pi_s < 110000Pa$. The maximum imaginary part of all eigenvalues and the maximum of real part of all eigenvalues as a function of π_s is plotted on Figure 9. We see that for the whole tested range of pressured the eigenvalues of FE laplacian are real and negative.

7.1 Eigenvalues of $C1$ constrain

This subsection is a bit out of topic, but is for those who are involved in model dynamics development.

The $C1$ constrain is defined as

$$C1 = -\mathbf{G}^* * \mathbf{S}^* + \mathbf{G}^* + \mathbf{S}^* - \mathbf{N}^*. \quad (14)$$

The \mathbf{G}^* operator is the vertical integral operator from model surface to model top. Its value at model top is unbounded as it project pressure levels into geopotential levels. And geopotential is unbounded at top of atmosphere.

The \mathbf{S}^* is vertical integral operator from model top to surface. The values of this operator are bounded and well defined. This operators transform local mass information into mass above specific place.

The operator \mathbf{N}^* is \mathbf{S}^* operator computed over the whole depth of atmosphere. Physically, this operator transform vertical profile of quantities into surface mass (pressure).

We have defined two sets of operators.

1. IntTop - the FE vertical integral operator from top to η with stiff matrix

$$\sum_{i=1}^L \int_0^1 \hat{\mathbf{f}}_i \left(\int_0^\eta \mathbf{B}_i(\tau) \mathbf{w}_j(\tau) d\tau \right) d\eta, \quad j = (1, \dots, L). \quad (15)$$

with boundary conditions $D_{top} = 0$ and $\frac{\partial B}{\partial \eta}_{top} = \frac{\partial B}{\partial \eta}_{surf} = 0$

2. IntBot - the FE vertical integral operator from surface to η with stiff matrix

$$\sum_{i=1}^L \int_0^1 \hat{\mathbf{f}}_i \left(\int_0^1 \mathbf{B}_i(\tau) \mathbf{w}_j(\tau) d\tau - \int_0^\eta \mathbf{B}_i(\tau) \mathbf{w}_j(\tau) d\tau \right) d\eta, \quad j = (1, \dots, L). \quad (16)$$

with boundary conditions $D_{surf} = 0$ and $\frac{\partial B}{\partial \eta}_{top} = \frac{\partial B}{\partial \eta}_{surf} = 0$.

The operators \mathbf{G}^* , \mathbf{S}^* and \mathbf{N}^* are then defined purely from one of them to ensure integration property $\int_0^1 f(\eta) d\eta = \int_0^\eta f(\eta) d\eta + \int_\eta^1 f(\eta) d\eta$.

The boundary condition imposed on input function $\frac{\partial B}{\partial \eta}_{top} = \frac{\partial B}{\partial \eta}_{surf} = 0$ is purely empirical. We try to control potential overshooting in extrapolated parts of domain.

The spectral radius of $C1$ computed with the two sets of operators, for the vertical levels settings described in previous section is plotted on Figure 10. It is apparent that the $C1$ expressed with FE integral operator starting from top has better properties.

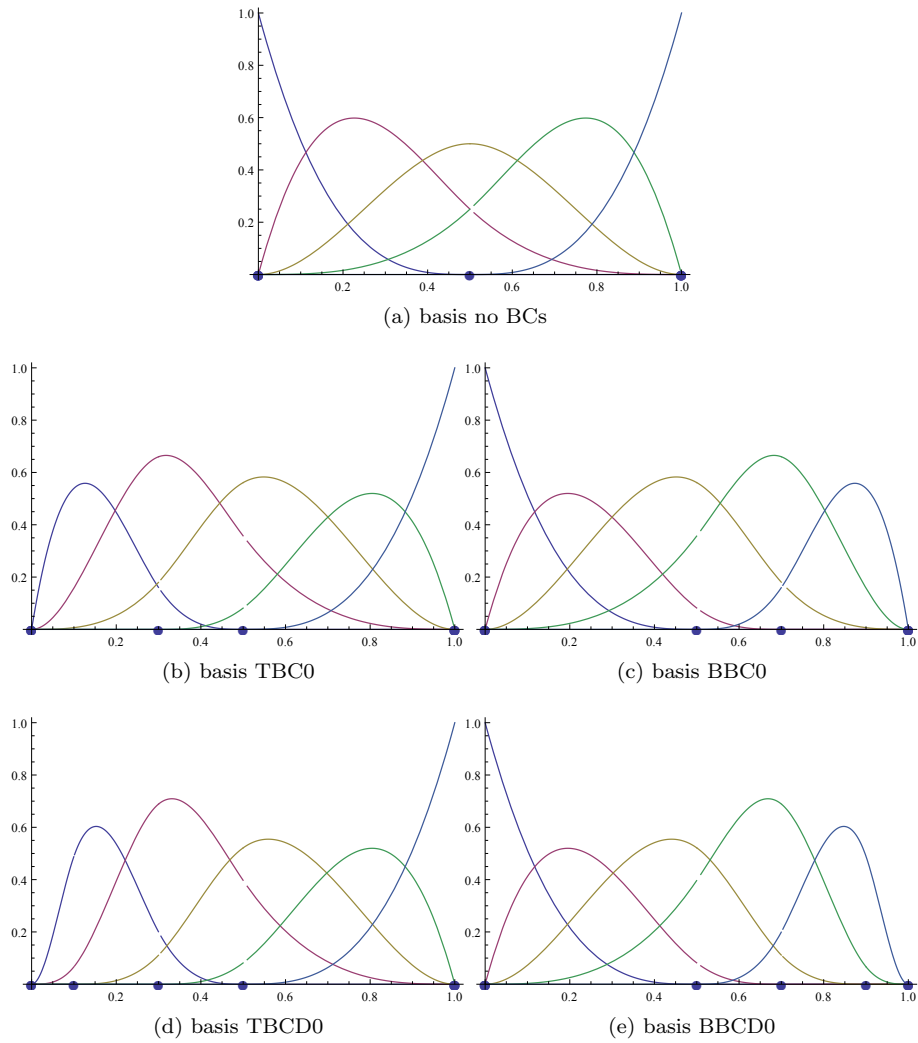


Figure 1: The basis functions for 5 regular levels and various multiplicity at boundaries. Using distinct set of basis functions we can control BCs of differential operator discretized using FE method.

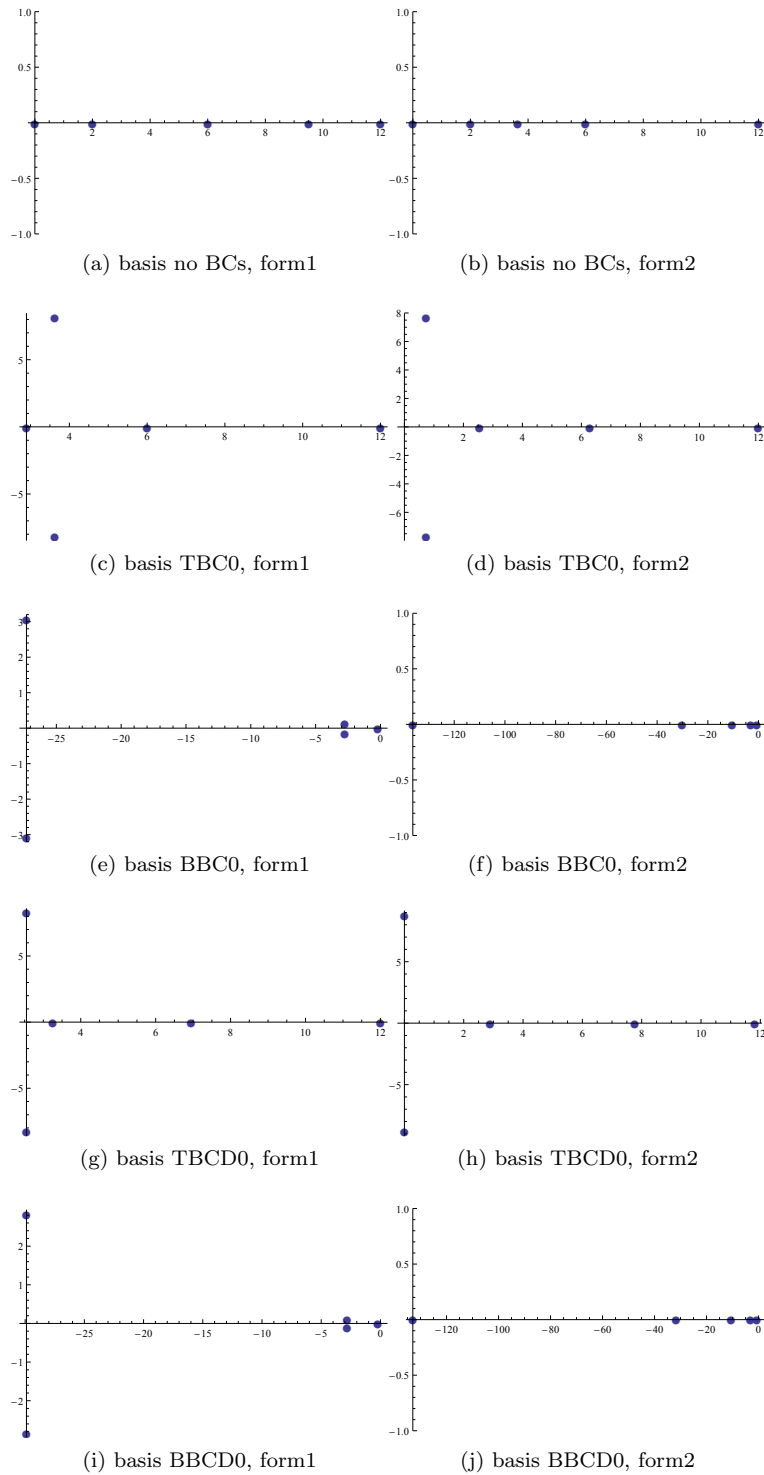


Figure 2: Eigenvalues in complex plane of laplacian operator discretized with FE method. Columns are two distinct formulations of laplacian operator, rows are basis functions with various BCs plotted on Figure 1

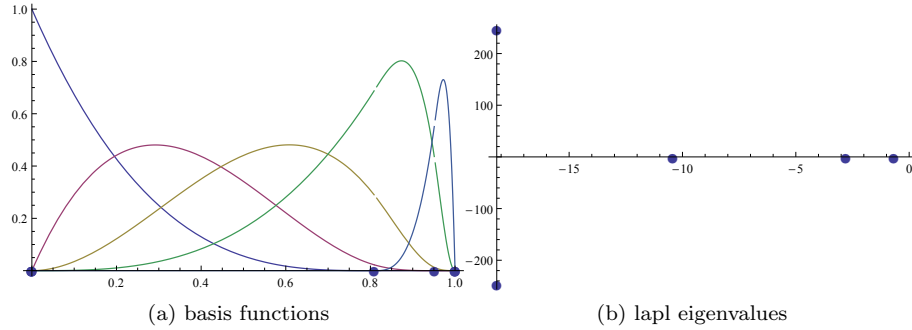


Figure 3: Cubic spline basis of knot sequence independent on full level values of η on the left, relevant eigenvalues of laplacian operator on the right.

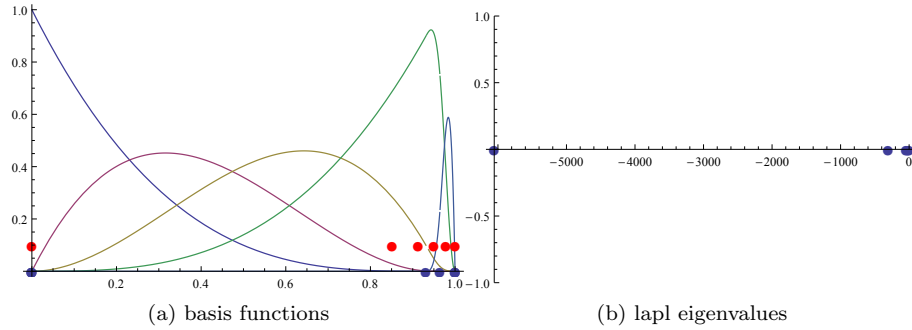


Figure 4: Cubic spline basis for non-regular levels $\sigma_{\bar{l}} = \left(\frac{\bar{l}}{L}\right)^{0.1}$ on the left and relevant eigenvalues of laplacian operator on the right. Red dots are half levels values of σ , dark dots are knots.

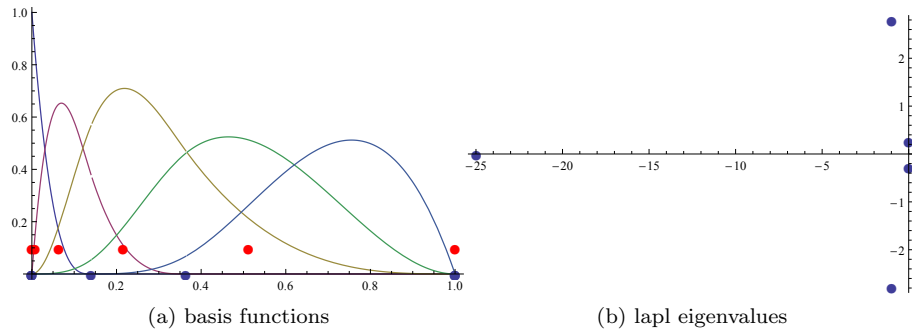


Figure 5: Cubic spline basis for non-regular levels $\sigma_{\bar{l}} = \left(\frac{\bar{l}}{L}\right)^3$ on the left and relevant eigenvalues of laplacian operator on the right. Red dots are half levels values of σ , dark dots are knots.

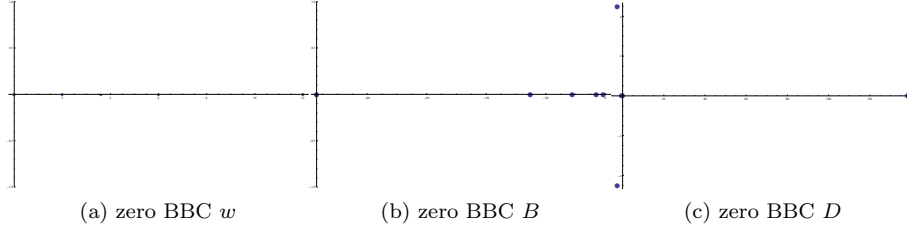


Figure 6: The eigenvalues of laplacian operator when zero BBC is applied only in one of spline basis.

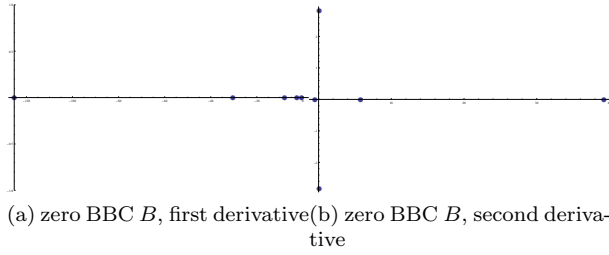


Figure 7: The eigenvalues of laplacian operator when zero BBC is imposed on B spline basis only in first derivative operator (left) and only in second derivative operator (right).

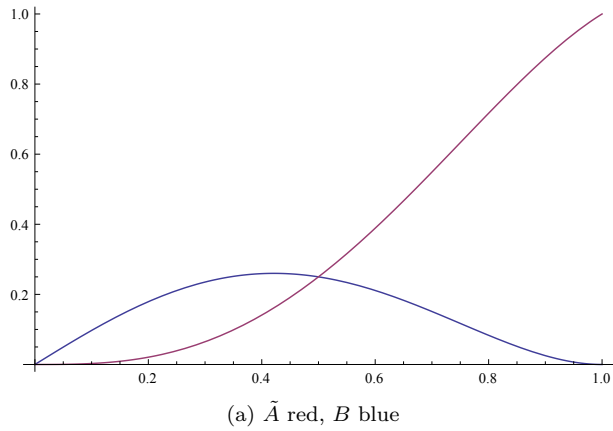


Figure 8: Our choice of $\tilde{A}(\eta)$ and B functions.

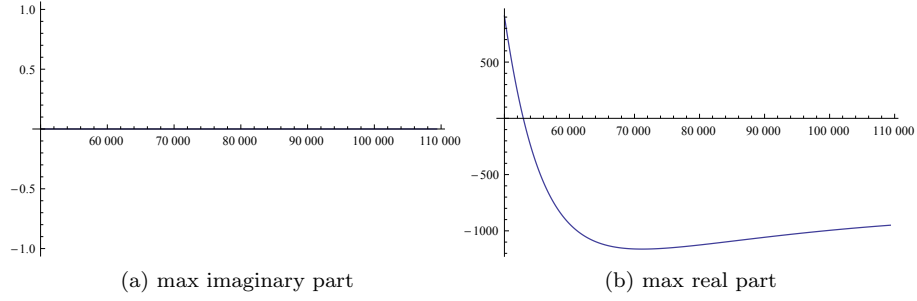


Figure 9: The maximum imaginary and real parts of eigenvalues of FE discretized laplacian operator for $50000Pa < \pi_s < 110000Pa$ computed with η coordinate. We use 15 non-regular levels and BBC 0 assumed for input quantity. This BBC is build implicitly inside the cubic spline basis functions B .

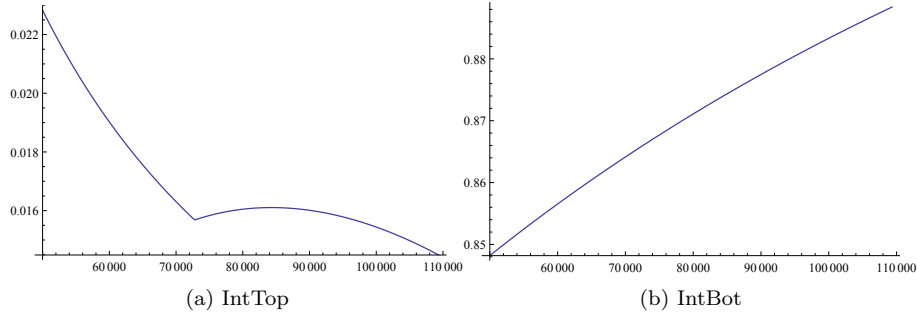


Figure 10: The spectral radius of $C1$ as a function of π_s for two different sets of integral operators with boundary conditions $\frac{\partial B}{\partial \eta_{top}} = \frac{\partial B}{\partial \eta_{surf}} = 0$